Simultaneous Optical and Radio Frequency Transmission Using Optical Phase Stabilization Combined With Phase Conjugation Technology

Lei Liu, Nan Cheng, JiangLiang Wang, Qian Cao, Zhou Tong, Kang Ying, and Youzhen Gui

***Abstract*—We propose and demonstrate a new simultaneous optical and radio frequency (RF) transmission scheme using optical phase stabilization combined with phase conjugate technology. The acousto-optical modulator (AOM) is used as a frequency actuator to compensate the optical frequency phase noise introduced by the optical fiber link, and the electro-optical modulator (EOM) is used to modulate two optical carrier sidebands simultaneously to stabilize the RF phase by phase conjugate technology. The novelty is that forward and backward RFs are distinguished by the AOMs used in standard optical carrier transfer to avoid the backscattering without WDM, so that the optical link is more symmetric, reducing the degradation of frequency stability due to polarization fluctuation and chromatic dispersion thermal sensitivity. We experimentally demonstrate 193.4 THz optical frequency transfer with a frequency stability of 1.2×10^{-17} at the integral time of 1 s and 3.3×10^{-19} at 10000 s, 1 GHz RF with a frequency stability of 7×10^{-13} at 1 s and 3×10^{-16} at 10000 s over a 50.4 km fiber spools. This novel scheme demonstrates the compatibility of two contrasting fiber noise cancellation techniques, and is superior to the current optical frequency and RF simultaneous transmission schemes in terms of cost and complexity.**

***Index Terms*—Optical frequency transfer, radio frequency transfer, simultaneous transfer.**

Manuscript received 11 July 2022; accepted 12 July 2022. Date of publication 18 July 2022; date of current version 28 July 2022. This work was supported in part by the National Key Research and Development Program of China under Grant 2020YFB0408300, in part by the National Natural Science Foundation of China under Grant 62175246, in part by the Natural Science Foundation of Shanghai under Grant 22ZR1471100, and in part by the Youth Innovation Promotion Association of the Chinese Academy of Sciences under Grant YIPA2021244. *(Corresponding author: Youzhen Gui.)*

Lei Liu is with the Key Laboratory for Quantum Optics, Shanghai Institute of Optics and Fine Mechanics, Chinese Academy of Sciences, Shanghai 201800, China, and also with the University of Chinese Academy of Sciences, Beijing 100049, China (e-mail: leil@siom.ac.cn).

Nan Cheng, JiangLiang Wang, Qian Cao, and Zhou Tong are with the Key Laboratory for Quantum Optics, Shanghai Institute of Optics and Fine Mechanics, Chinese Academy of Sciences, Shanghai 201800, China (e-mail: chengnan98@siom.ac.cn; jialiangking@siom.ac.cn; caoqian@siom.ac.cn; tz2020@siom.ac.cn).

Kang Ying is with the Key Laboratory of Space Laser Communication and Detection Technology, Shanghai Institute of Optics and Fine Mechanics, Chinese Academy of Sciences, Shanghai 201800, China (e-mail: yingk0917@siom.ac.cn).

Youzhen Gui is with the Key Laboratory for Quantum Optics, Shanghai Institute of Optics and Fine Mechanics, Chinese Academy of Sciences, Shanghai 201800, China, with the University of Chinese Academy of Sciences, Beijing 100049, China, and also with the Center of Materials Science and Optoelectronics Engineering, University of Chinese Academy of Sciences, Beijing 100049, China (e-mail: yzgui@siom.ac.cn).

Digital Object Identifier 10.1109/JPHOT.2022.3191320

I. Introduction

HIGH-precision frequency standards have been playing an important role in various research fields such as: fundamental physics [1], [2] (e.g., search for dark matter and general relativity effect verification [3]–[5], optical clock comparison [6]–[8]), radio astronomy [9], positioning and navigation timing [10], [11]. The low-noise optical frequency transmission has the best performance because of its high carrier frequency and no fiber chromatic dispersion effect [12]–[18], but most practical applications still require the transmission of stable radio or microwave frequency to interface with electronic system [19], [20]. Optical frequency and RF simultaneous dissemination methods has been developed rapidly including optical frequency comb [19], [21], dual-optical stabilization technique [20], [22], and the hybrid solution combining interferometric stabilization with the electronically stabilized (ELSTAB) technology [23], [24]. However, the optical frequency comb is too expensive, large and complex [25], [26]. Although the dual-optical stabilization technique is an efficient choice, the method of Gozzard *et al.* may induce uncommon-mode phase noise on stable RF since the two optical frequencies go through different optical paths at the local site and two independently active compensation devices are used [20]. Similarly, the method of Tian *et al.* can compensate the phase noise of two optical frequencies simultaneously by using one optical actuator. This method simplifies the number of compensation optical actuators and achieves dual optical frequencies and RF simultaneous transmission [22]. However, it still requires two optical phase stabilization devices and adds a phase-locked dielectric resonator oscillator to increase the interval frequency between optical frequencies. The two independent optical phase stabilization devices introduce uncommon-mode phase noise into the stable RF. In addition, the hybrid solution for the optical frequency and RF simultaneous transmission requires two independent systems to process the optical and RF signals separately, which increases the complexity of system. And the solution also requires two wavelengths on forward and backward directions to avoid the backscattering effect on the RF transfer stability.

We propose a scheme to achieve optical frequency and RF simultaneous transmission, which uses only a single set of standard optical frequency phase stabilization devices combined with phase conjugation technology to suppress the phase noise introduced by the optical fiber link. Different from conventional

RF transfer by phase conjugation techniques [27], [28], microwave frequency mixers circuits is designed to help obtain the backward RF without WDM (no need to use different channel wavelengths), so that the frequency stability of RF signal is not affected by the backscattering and optical frequency, and it is also not greatly affected by the chromatic dispersion effect [29]. The proposed scheme requires phase conjugation setup, but the passive components, such as mixers, are more reliable than the active ones. Thus the scheme shares several attributes with optical frequency transfer, and simplifies the phase noise compensation devices.

The paper is organized as follows: Section II describes the details of the proposed the optical frequency and RF simultaneous transmission technique. In Section III, the experimental apparatus and the main results are introduced, including the evaluation performance of optical frequency and RF transmission. The Section IV mainly discusses the limitations of the current system and the feasible schemes for future improvement. Finally, the conclusion is given in the Section V.

II. Principle of Optical Frequency and Radio Frequency Transmission System

The basic idea is to use a single set of standard optical phase stabilization device to simultaneously transmit stable optical frequency and RF. The phase noise of optical frequency and RF needs to be compensated simultaneously using Doppler noise suppression and phase conjugate technique to implement this idea. Therefore, the EOM needs to be driven by two RFs with angular frequencies Ω_1 andΩ_2, where Ω_1 is a local RF signal and Ω_2 is a phase conjugate RF signal carrying the round-trip phase noise of fiber link (that will be mentioned later). In the proposed scheme, the local AOM used in standard optical carrier transfer is used to compensate for optical frequency jitter. The local and remote AOMs are used not only to distinguish forward and backward optical frequency signals, but also to distinguish the forward and backward RFs. Therefore, the novel method uses single standard phase noise compensation, so the advantages of optical frequency propagation can be utilized to reduce the cost, size and complexity of stabilizing equipment.

Fig. 1 illustrates a schematic view of the technical principle of optical frequency and RF simultaneous transmission system. In the paper here and below, the amplitude and initial phase are omitted for clarity.

The reference optical carrier $\mathrm{E}_0 \propto \cos(\omega_0 t)$from a laser is fed into an EOM (Mach-Zehnder style) biased at $\mathrm{V}_\pi/2$. Thus the modulated optical carrier has two double first-order sidebands (Ω_1 and Ω_2), corresponding to two RF signals, with angular frequencies $\omega_0 + \Omega_1$ and $\omega_0 + \Omega_2$ (only the upper sidebands are considered for clarity). The modulated output optical signal by EOM can be expressed as:

$$\mathrm{E}_1 \propto \cos(\omega_0 \mathrm{t}) + \cos(\omega_0 \mathrm{t} + \Omega_1 \mathrm{t}) + \cos(\omega_0 \mathrm{t} + \Omega_2 \mathrm{t}) \quad (1)$$

where ω_0 is the angular frequency of the optical carrier; Ω_1 is the stable RF from multichannel DDS and Ω_2 is the phase conjugate RF with round-trip phase noise.

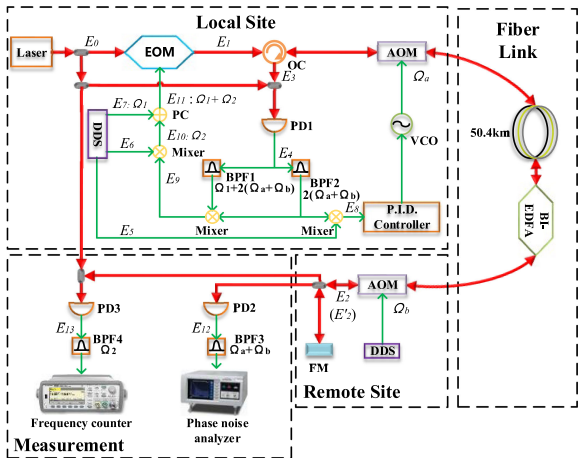

Fig. 1. Schematic diagram of the technical principle of fiber-optic optical frequency and Radio frequency simultaneous transmission system. EOM: electro-optic modulator, OC: optical circulator, AOM: acousto-optic modulator, BI-EDFA: bidirectional erbium-doped fiber amplifier, PD: photodetector, PC: Power combiner, VCO: voltage-controlled oscillator, DDS: direct-digital synthesizer, BPF: band-pass filter, PID: proportional-integral-derivative controller, FM: Faraday mirror.

The modulated optical signal is fed into the local AOM through the optical circulator. Different optical frequencies accumulate different phase fluctuations from environmental perturbations when the optical frequencies pass through the same fiber link. At the remote site, the optical signal goes through a remote AOM to separate the required round-trip signal from the spurious reflections on the fiber link, and then the optical signal becomes:

$$\begin{aligned}\mathrm{E}_2 \propto\ & \cos[(\omega_0 + \Omega_\mathrm{a})(\mathrm{t} - \Delta\mathrm{t}) + \Omega_\mathrm{b}\mathrm{t} + \varphi_{\Omega_\mathrm{a}} + \varphi_{\Omega_\mathrm{b}}] \\ & + \cos[(\omega_0 + \Omega_\mathrm{a} + \Omega_1)(\mathrm{t} - \Delta\mathrm{t}) + \Omega_\mathrm{b}\mathrm{t} + \varphi_{\Omega_\mathrm{a}} + \varphi_{\Omega_\mathrm{b}}] \\ & + \cos[(\omega_0 + \Omega_\mathrm{a} + \Omega_2)(\mathrm{t} - \Delta\mathrm{t}) + \Omega_\mathrm{b}\mathrm{t} + \varphi_{\Omega_\mathrm{a}} + \varphi_{\Omega_\mathrm{b}}]\end{aligned} \quad (2)$$

where Ω_a and Ω_b are the operating frequencies of the local and remote AOM respectively; $\varphi_{\Omega_\mathrm{a}}$and $\varphi_{\Omega_\mathrm{b}}$ are the phase shifts introduced when the optical signal passes through different AOM; $\Delta\mathrm{t}$ represents the transmission delay time introduced by optical fiber link.

At the remote site, the optical signal is split into two paths, one path of optical signal enters the PD2 and PD3 (beats with reference optical carrier), respectively, the other is reflected back to the local site along the same fiber link through the Faraday mirror at the remote site and is received by the PD1. Assuming that the forward and backward optical signals experience the same phase fluctuations, the round-trip optical signals can be described as:

$$\begin{aligned}\mathrm{E}_3 \propto\ & \cos \\ & [\omega_0(\mathrm{t} - 2\Delta\mathrm{t}) + 2(\Omega_\mathrm{a} + \Omega_\mathrm{b})(\mathrm{t} - \Delta\mathrm{t}) + 2\varphi_{\Omega_\mathrm{a}} + 2\varphi_{\Omega_\mathrm{b}}] \\ & + \cos[(\omega_0 + \Omega_1)(\mathrm{t} - 2\Delta\mathrm{t}) + 2(\Omega_\mathrm{a} + \Omega_\mathrm{b})(\mathrm{t} - \Delta\mathrm{t}) \\ & + 2\varphi_{\Omega_\mathrm{a}} + 2\varphi_{\Omega_\mathrm{b}}] + \cos[(\omega_0 + \Omega_2)(\mathrm{t} - 2\Delta\mathrm{t}) \\ & + 2(\Omega_\mathrm{a} + \Omega_\mathrm{b})(\mathrm{t} - \Delta\mathrm{t}) + 2\varphi_{\Omega_\mathrm{a}} + 2\varphi_{\Omega_\mathrm{b}}]\end{aligned} \quad (3)$$

E_3 beats with E_0 on PD1, whose output can be described as:

$$\begin{aligned} E_4 \propto & \cos[2(\Omega_a+\Omega_b)t - 2(\omega_0+\Omega_a+\Omega_b)\Delta t \\ & + 2\varphi_{\Omega_a} + 2\varphi_{\Omega_b}] + \cos\{[\Omega_1 + 2(\Omega_a+\Omega_b)]t \\ & - 2(\omega_0+\Omega_1+\Omega_a+\Omega_b)\Delta t + 2\varphi_{\Omega_a} + 2\varphi_{\Omega_b}\} \\ & + \cos\{[\Omega_2 + 2(\Omega_a+\Omega_b)]t - 2(\omega_0+\Omega_2 \\ & + \Omega_a+\Omega_b)\Delta t + 2\varphi_{\Omega_a} + 2\varphi_{\Omega_b}\} \end{aligned} \quad (4)$$

To assist in acquiring the error frequency signal with phase noise introduced by the fiber link, three RF signals need to be generated at the local site using a multichannel DDS.

$$E_5 \propto \cos[2(\Omega_a+\Omega_b)t] \quad (5)$$

$$E_6 \propto \cos(3\Omega_1 t) \quad (6)$$

$$E_7 \propto \cos(\Omega_1 t) \quad (7)$$

Mixing E_5 with the first term of E_4, and taking the low-frequency components by band-pass filtering, the error signal is obtained, which is identical with standard optical carrier transfer:

$$E_8 \propto \cos[2(\omega_0+\Omega_a+\Omega_b)\Delta t - 2\varphi_{\Omega_a} - 2\varphi_{\Omega_b}] \quad (8)$$

Mixing the two RFs of the first and second terms in E_4 to obtain E_9, it contains the RF phase noise that excludes optical frequency phase noise. And taking the low-frequency products and E_9 can be obtained:

$$E_9 \propto \cos(\Omega_1 t - 2\Omega_1 \Delta t) \quad (9)$$

It should be noted that direct detection can be understood as beating between the sidebands and the center frequency, and in this sense E_9 is equivalent to direct detection of the round-trip optical signals. However, since the forward transmitted frequency signal has the same angular frequency as E_9 and these propagate on the same wavelength, the signal obtained by direct detection is interfered by the backward scattering [30]. This way of the E_9 obtained by the designed microwave frequency mixers circuits avoids that problem.

Then, E_9 is mixed with E_6 (third harmonic of Ω_1) to obtain phase conjugation signal E_{10} with the angular frequency Ω_2 (that means the Ω_2 mentioned above that is fed into the EOM equals E_{10}):

$$E_{10} \propto \cos(2\Omega_1 t + 2\Omega_1 \Delta t) \quad (10)$$

The signals E_{10} (at angular frequency $2\Omega_1$) and E_7 (at angular frequency Ω_1) are combined in the adder and fed to the EOM.

$$E_{11} \propto \cos(\Omega_1 t) + \cos(2\Omega_1 t + 2\Omega_1 \Delta t) \quad (11)$$

For compensating optical frequency phase noise, the error signal E_8 is fed into the voltage controlled oscillator (VCO) after proportional integral differentiation (PID). Thus, adjusting φ_{Ω_a} can compensate the phase noise introduced by optical fiber link.

$$\varphi_{\Omega_a} = (\omega_0+\Omega_a+\Omega_b)\Delta t - \varphi_{\Omega_b} \quad (12)$$

Substituting the φ_{Ω_a}, $\Omega_2 t = 2\,\Omega_1 t + 2\Omega_1 \Delta t$ and $\Omega_2 \Delta t = 2\,\Omega_1 \Delta t$ into E_2 (because angular frequency Ω_2 equals angular frequency $2\Omega_1$), the remote site result can be expressed as:

$$\begin{aligned} E_2' \propto & \cos[(\omega_0+\Omega_a+\Omega_b)t + \Omega_b \Delta t] \\ & + \cos[(\omega_0+\Omega_a+\Omega_b+\Omega_1)t - \Omega_1 \Delta t + \Omega_b \Delta t] \\ & + \cos[(\omega_0+\Omega_a+\Omega_b+2\Omega_1)t + \Omega_b \Delta t] \end{aligned} \quad (13)$$

The E_2' contains the stable optical frequency and RF after phase noise compensation. Here we note the existence of residual phase noise $\Omega_b \Delta t$. Since the frequency stability of optical frequency can be calculated from $\partial((\omega+\Omega_b)\Delta t)/\omega \partial t$, this residual phase noise $\Omega_b \Delta t$ is six orders of magnitude smaller than the phase noise $\omega_0 \Delta t$, its effect on the stabilized optical frequency can be neglected [22].

At the moment, a stable RF signal can be obtained on PD2 by direct detection E_2' and band pass filtering for angular frequency $2\Omega_1$. It also be noted that direct detection is equivalent to beating both the higher sideband and the lower sideband with the carrier, but the cancellation of phase noise works also for the lower sideband.

$$E_{12} = \cos(2\Omega_1 t) \quad (14)$$

In order to evaluate the performance of RF transfer effectively, the E_{12} is evaluated through phase noise analyzer. For the same purpose, E_2' beats with the reference optical carrier to get E_{13} on PD3. In other words, the stability of optical frequencies can be effectively evaluated by filtering and monitoring the E_{13} through frequency counter.

$$E_{13} = \cos[(\Omega_a+\Omega_b)t + \Omega_b \Delta t] \quad (15)$$

III. Construction of Experimental Apparatus and Results

A. Experimental Apparatus

To verify the principle of the above proposed scheme, the optical frequency and RF simultaneous transmission system over 50.4 km fiber spools was built. To facilitate the evaluation of the system performance, the local and remote sites are placed together so that the frequency stability of the optical frequency and RF can be measured simultaneously. The optical signal being fed to the EOM is generated by the NKT-X15 narrow linewidth laser, which has a wavelength $\lambda = 1550.12$ nm and the linewidth of less than 100 Hz. The bandwidth of the EOM is 10 GHz and its bias point is set at$V_\pi/2$ with an insertion loss of 9 dBm. To avoid Brillouin scattering and other nonlinear effects [31], the optical signal power fed to the fiber link is kept at a low level (about 0 dBm in our example). Considering the experimental equipment in our laboratory, we chose the frequency of $\Omega_1 = 500$ MHz, the stable 1 GHz RF signal ($E_{12} = \cos(2\Omega_1 t)$) will be obtained in our experiment results. The local and remote AOMs are driven by the same frequency $\Omega_a = \Omega_b = 75$ MHz (downshift mode, 1 order), and the local AOM is used to compensate the phase noise of optical carrier, while the remote AOM is used for distinguishing the reflected optical signal comes from the FM.

A bidirectional erbium-doped fiber amplifier (EDFA) is used to compensate for insertion loss due to EOM and other optical

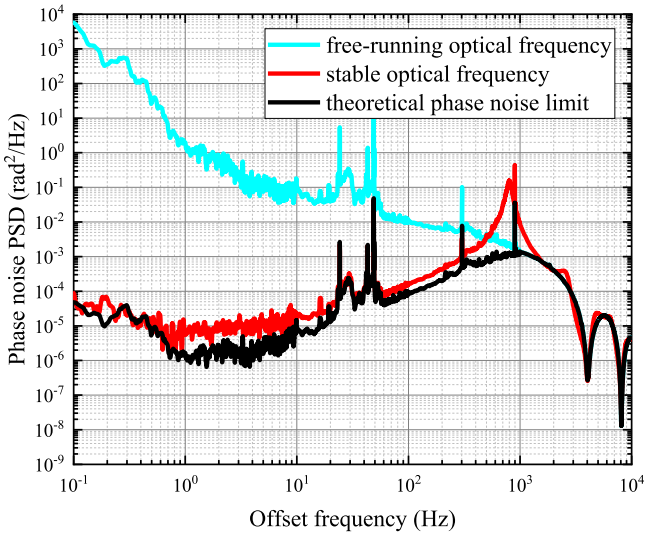

Fig. 2. Phase noise PSD of the free-running optical frequency (cyan) and the stabilized optical frequency (red) with the phase noise compensation scheme. The black curve is the theoretical prediction result Refer to (16).

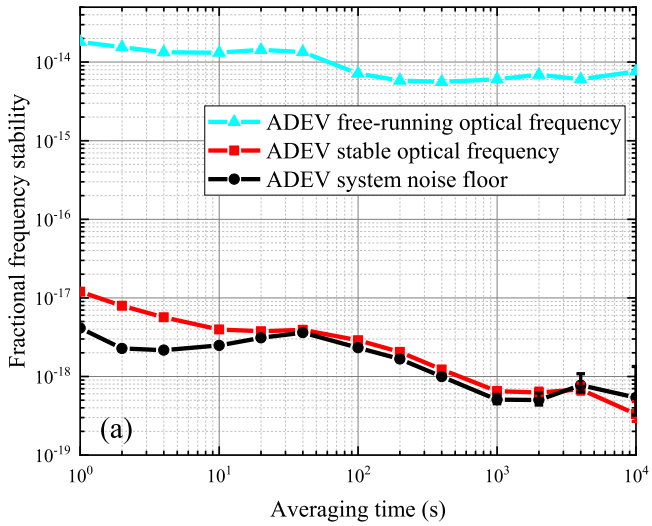

Fig. 3. Fractional frequency stability of the free-running optical frequency (cyan triangle) and the stabilized optical frequency (red plaid). The noise floor of the system is also shown (black circle).

devices, fiber link loss. We use frequency counter 53230A (lambda counting) [32], [33] and phase noise analyzer TSC 5125A to evaluate the stability of optical frequency and RF at the remote site. The local DDS generator is HS9004B with four-channel and channel-to-channel stability about 1×10^{-13} at 1 s.

In addition, the reference frequency source of all experimental devices are synchronized with the 10 MHz RF signal from REFGEN 10292 with the short-term stability 2×10^{-12} at 1 s to ensure the homology of the experimental devices.

B. Optical Frequency and RF Transfer Results

The ability to suppress the phase noise introduced by the fiber link is the core index to characterize the system performance. The optical frequency stability can be inferred from phase noise. Therefore, measuring the phase noise of the optical fiber link is a critical index for subsequent evaluation of link quality and the performance of the system.

Fig. 2 shows the free-running, stabilized and theoretical limitation phase noise of the optical frequency respectively. The cyan curve indicates the phase noise of the optical frequency when the noise compensation system is not operated, the red curve indicates the phase noise of the optical frequency when the noise compensation system works, and the black curve indicates the theoretical phase noise limit of the optical frequency.

As can be observed from the Fig. 2, when the noise compensation system starts to work, the phase noise PSD within the feedback bandwidth $1/4\tau$ is in good agreement with the theoretical prediction result, indicating that phase noise compensation system has worked well. The theoretical limited phase noise based on optical frequency transfer is presented [14]:

$$S_{\text{Stab}\_\varphi}(f) = \frac{1}{3}(2\pi f\tau)^2 S_{\text{Free}\_\varphi}(f) \tag{16}$$

where $S_{\text{Stab}\_\varphi}(f)$ and $S_{\text{Free}\_\varphi}(f)$ are the phase noises of the theoretical limit and the free-running case respectively, and τ is the time for the optical signal to be transmitted along the optical fiber link. We also observe that the phase noise of the optical frequency has a bump at the feedback bandwidth, which may be caused by the time delay or PID control part of the system.

The frequency stability of the optical frequency is shown in Fig. 3. The cyan triangle line indicates the frequency stability of the optical frequency in the free-running fiber link. The red plaid line indicates the frequency stability of the optical frequency in the stabilized state. The black circle line indicates the noise floor of the system. This system achieves stable optical frequency transfer over the 50.4 km fiber spools, with frequency stability of 1.2×10^{-17} at 1 s and 3.3×10^{-19} at 10000 s. With the phase noise compensation in operation, the system provides excellent suppression of fiber link phase noise and improves the stability by three orders of magnitude compared to the free-running fiber link. To test the phase noise floor of the system, a 1 m short fiber was used in place of the 50.4 km spools to measure the frequency stability at the remote site, and the optical frequency stability of 4.2×10^{-18} at 1 s and 5.5×10^{-19} at 10000 s is obtained. The experimental results of optical frequency stability are two orders of magnitude better than the results in [22], and the performance of the optical frequency stability is as good as those of conventional optical carrier transmission[12]–[18].

Fig. 4 shows the frequency stability of the RF at the remote site (BW = 0.5 Hz). The cyan triangle line is the performance of the 1 GHz RF in the free-running state. The red plaid line is the frequency stability of the RF in the stabilized state. The black circle line is the noise floor of the system. The results show that this system can achieve stable RF transmission with frequency stability 7×10^{-13} at 1 s and 3×10^{-16} at 10000 s over the 50.4 km fiber spools.

The phase noise PSD of the free-running and stable 1 GHz RF at the remote site also are shown in Fig. 5. The cyan curve is the phase noise of the RF in the free-running state, and the red curve

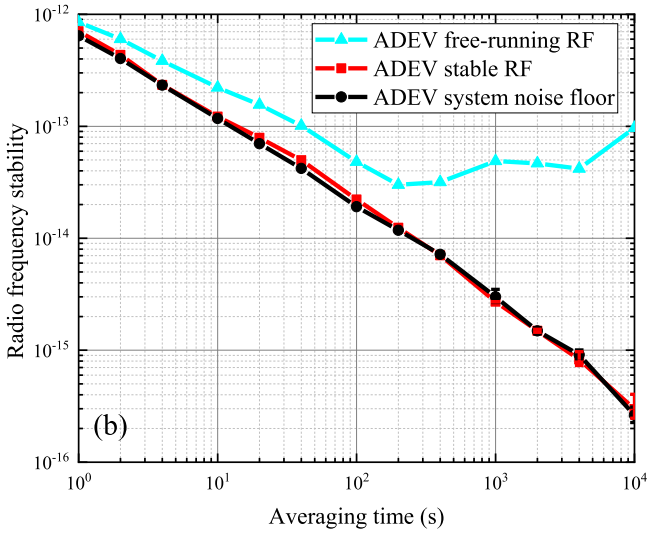

Fig. 4. Frequency stability of the free-running RF signal (cyan triangle) and the stabilized RF signal (red plaid). The noise floor of the RF signal is also shown (black circle).

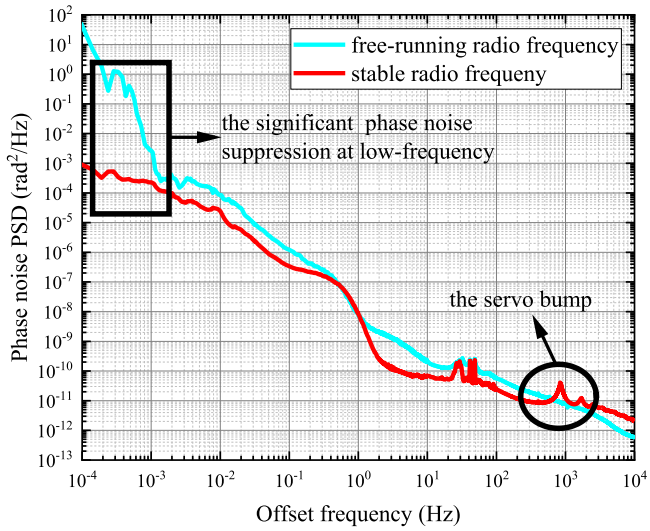

Fig. 5. Phase noise PSD of the free-running RF (cyan) and stabilized RF with phase noise compensation (red).

is the phase noise of the RF signal in the stabilized state. The phase noise of free-running RF within the feedback bandwidth is higher than the stabilized RF due to ambient temperature, vibration, and other factors. The clear servo bump still exists in the feedback bandwidth $1/4\tau$, and the phase noise PSD of the 1 GHz RF is suppressed significantly at low-frequency range, which is consistent with the long-term stability of the 1GHz RF as shown in Fig. 4. Compare the experimental results of RF frequency stability with the presented in [20], the stable RF frequency stability has obvious improvement with the free-running case in long term instability. However, we have to note that the experimental results of RF frequency stability is inconsistent with conventional RF transmission by amplitude modulating a continuous wave laser, in which RF frequency stability have significantly difference when the fiber phase stabilization devices starts to work or not [34], [35]. The main cause of this situation may be limited by the crosstalk phase noise effect or the experimental environment.

IV. Discussion

We propose and demonstrate the method of using single standard optical frequency phase stabilization devices and phase conjugate technology to realize optical frequency and RF simultaneous transmission. The scheme shares several attributes with optical frequency transfer, which greatly simplifies the simultaneous transmission system, and reduces the non-reciprocal noise due to polarization fluctuation and chromatic dispersion thermal sensitivity. And compare the dual-optical stabilization technique, the proposed scheme can avoid the accumulation of uncommon-mode residual noise on the RF from two independent active phase noise compensation devices. This means that the RF of the dual-optical stabilization technique receives the uncommon-mode residual noise of two independent noise compensation devices due to the RF signal is obtained by two stable optical frequency signal.

Benefitting from the modulation characteristics of EOM, the frequency stability of the RF signal may be improved by injecting more stable RF modulated frequency without affecting the optical frequency transmission performance. The above experimental results also show that the stability of the RF transfer is entirely dominated by the system noise floor. In the future, we will investigate the factors that limit RF frequency stability.

Although optical carrier transfer technology achieves the best fractional frequency stability, the existing frequency standards are still dominated by microwave atomic clocks, and many applications in science, commerce, and industry require a stable RF source for their systems. The proposed scheme can provide both RF and optical frequency, enabling a flexible link for a large number of applications mentioned above. This scheme is also beneficial to the construction of multiple RF signals joint transfer, which can simplify the complexity of the central site, reduces the difficulty of system maintenance.

V. Conclusion

We propose a scheme that simultaneous optical frequency and RF transmission can be realized in a simple way by using optical phase stabilization combined with phase conjugate technology. The key merit of the scheme is to utilize EOM as RF phase conjugate actuator and use only a single set of standard optical phase noise compensation device. The forward and backward RFs can be distinguished by the AOMs used in standard optical carrier transfer, so that the optical link is the optical link is more symmetric, reducing the degradation of frequency stability due to polarization fluctuation and chromatic dispersion thermal sensitivity. The novel scheme also demonstrates the compatibility of two contrasting fiber noise cancellation techniques. The experimental results show that the stable transmission of optical frequency and RF over 50.4 km fiber spools is achieved. The frequency stability of 193.4 THz optical frequency at the remote site is 1.2×10^{-17} at 1 s and 3.3×10^{-19} at 10000 s, the frequency stability of 1 GHz RF is

7×10^{-13} at 1 s and 3×10^{-16} at 10000 s. This scheme can simultaneously provide stable optical frequency and RF references for remote users. It can be used in optical clock comparison, geodesy, and other fundamental physics experiments.

REFERENCES

[1] C. Lisdat *et al.*, "A clock network for geodesy and fundamental science," *Nature Commun.*, vol. 7, Aug. 2016, Art. no. 12443.

[2] S. Schiller *et al.*, "Einstein gravity explorer–A medium-class fundamental physics mission," *Exp. Astron.*, vol. 23, no. 2, pp. 573–610, 2009.

[3] S. Kolkowitz, I. Pikovski, N. Langellier, M. D. Lukin, R. L. Walsworth, and J. Ye, "Gravitational wave detection with optical lattice atomic clocks," *Phys. Rev. D*, vol. 94, no. 12, 2016, Art. no. 124043.

[4] C.-W. Chou, D. B. Hume, T. Rosenband, and D. J. Wineland, "Optical clocks and relativity," *Science*, vol. 329, no. 5999, pp. 1630–1633, 2010.

[5] B. M. Roberts *et al.*, "Search for transient variations of the fine structure constant and dark matter using fiber-linked optical atomic clocks," *New J. Phys.*, vol. 22, no. 9, Sep. 2020, Art. no. 093010.

[6] W.-K. Lee, F. Stefani, A. Bercy, O. Lopez, A. Amy-Klein, and P.-E. Pottie, "Hybrid fiber links for accurate optical frequency comparison," *Appl. Phys. B-Lasers Opt.*, vol. 123, no. 5, May 2017, Art. no. 161.

[7] M. I. Bodine *et al.*, "Optical atomic clock comparison through turbulent air," *Phys. Rev. Res.*, vol. 2, no. 3, 2020, Art. no. 033395.

[8] W. F. McGrew *et al.*, "Towards the optical second: Verifying optical clocks at the SI limit," *Optica*, vol. 6, no. 4, pp. 448–454, 2019.

[9] B. Wang, X. Zhu, C. Gao, Y. Bai, J. Dong, and L. Wang, "Square kilometre array telescope—Precision reference frequency synchronisation via 1f-2f dissemination," *Sci. Rep.*, vol. 5, no. 1, pp. 1–7, 2015.

[10] W. McGrew *et al.*, "Atomic clock performance enabling geodesy below the centimetre level," *Nature*, vol. 564, no. 7734, pp. 87–90, 2018.

[11] C. Clivati *et al.*, "A VLBI experiment using a remote atomic clock via a coherent fibre link," *Sci. Rep.*, vol. 7, Feb. 2017, Art. no. 40992.

[12] L. S. Ma, P. Jungner, J. Ye, and J. L. Hall, "Delivering the same optical frequency at 2 places-accurate cancellation of phase noise introduced by an optical-fiber or other time-varying path," *Opt. Lett.*, vol. 19, no. 21, pp. 1777–1779, Nov. 1994.

[13] S. M. Foreman, A. D. Ludlow, M. H. G. de Miranda, J. E. Stalnaker, S. A. Diddams, and J. Ye, "Coherent optical phase transfer over a 32-km fiber with 1 s instability at 10(-17)," *Phys. Rev. Lett.*, vol. 99, no. 15, Oct. 2007, Art. no. 153601.

[14] P. A. Williams, W. C. Swann, and N. R. Newbury, "High-stability transfer of an optical frequency over long fiber-optic links," *J. Opt. Soc. Amer. B-Opt. Phys.*, vol. 25, no. 8, pp. 1284–1293, Aug. 2008.

[15] C. Clivati *et al.*, "Optical frequency transfer over submarine fiber links," *Optica*, vol. 5, no. 8, pp. 893–901, Aug. 2018.

[16] K. Predehl *et al.*, "A 920-kilometer optical fiber link for frequency metrology at the 19th decimal place," *Science*, vol. 336, no. 6080, pp. 441–444, 2012.

[17] S. Droste *et al.*, "Optical-frequency transfer over a single-span 1840 km fiber link," *Phys. Rev. Lett.*, vol. 111, no. 11, Sep. 2013, Art. no. 110801.

[18] D. Calonico *et al.*, "High-accuracy coherent optical frequency transfer over a doubled 642-km fiber link," *Appl. Phys. B-Lasers Opt.*, vol. 117, no. 3, pp. 979–986, Dec. 2014.

[19] S. M. Foreman, K. W. Holman, D. D. Hudson, D. J. Jones, and J. Ye, "Remote transfer of ultrastable frequency references via fiber networks," *Rev. Sci. Instruments*, vol. 78, no. 2, 2007, Art. no. 021101.

[20] D. R. Gozzard, S. W. Schediwy, and K. Grainge, "Simultaneous transfer of stabilized optical and microwave frequencies over fiber," *IEEE Photon. Technol. Lett.*, vol. 30, no. 1, pp. 87–90, Jan. 2018.

[21] G. Marra *et al.*, "High-resolution microwave frequency transfer over an 86-km-long optical fiber network using a mode-locked laser," *Opt. Lett.*, vol. 36, no. 4, pp. 511–513, 2011.

[22] X. Tian, L. Hu, G. Wu, and J. Chen, "Hybrid fiber-optic radio frequency and optical frequency dissemination with a single optical actuator and dual-optical phase stabilization," *J. Lightw. Technol.*, vol. 38, no. 16, pp. 4270–4278, Aug. 2020.

[23] P. Krehlik, H. Schnatz, and Ł. Śliwczyński, "A hybrid solution for simultaneous transfer of ultrastable optical frequency, RF frequency, and UTC time-tags over optical fiber," *IEEE Trans. Ultrasonics Ferroelect. Freq. Control*, vol. 64, no. 12, pp. 1884–1890, Dec. 2017.

[24] P. Krehlik, Ł. Śliwczyński, Ł. Buczek, H. Schnatz, and J. Kronjäger, "Optical multiplexing of metrological time and frequency signals in a single 100-GHz-Grid optical channel," *IEEE Trans. Ultrasonics Ferroelect. Freq. Control*, vol. 68, no. 6, pp. 2303–2310, Jun. 2021.

[25] T. Udem, R. Holzwarth, and T. W. Hänsch, "Optical frequency metrology," *Nature*, vol. 416, no. 6877, pp. 233–237, 2002.

[26] D. J. Jones *et al.*, "Carrier-envelope phase control of femtosecond mode-locked lasers and direct optical frequency synthesis," *Science*, vol. 288, no. 5466, pp. 635–639, 2000.

[27] C. Liu *et al.*, "Stabilized radio frequency transfer via 100 km urban optical fiber link using passive compensation method," *IEEE Access*, vol. 7, pp. 97487–97491, 2019.

[28] Y. He *et al.*, "Stable radio-frequency transfer over optical fiber by phase-conjugate frequency mixing," *Opt. Exp.*, vol. 21, no. 16, pp. 18754–18764, 2013.

[29] O. Lopez, A. Amy-Klein, M. Lours, C. Chardonnet, and G. Santarelli, "High-resolution microwave frequency dissemination on an 86-km urban optical link," *Appl. Phys. B*, vol. 98, no. 4, pp. 723–727, 2010.

[30] Ł. Śliwczyński, P. Krehlik, and M. Lipiński, "Optical fibers in time and frequency transfer," *Meas. Sci. Technol.*, vol. 21, no. 7, 2010, Art. no. 075302.

[31] M. Ferreira, J. Rocha, and J. Pinto, "Analysis of the gain and noise characteristics of fibre brillouin amplifiers," *Opt. Quantum Electron.*, vol. 26, no. 1, pp. 35–44, 1994.

[32] T. Dunker, H. Hauglin, and O. P. Rønningen, "On temporal correlations in high-resolution frequency counting," in *Proc. Eur. Freq. Time Forum*, 2016, pp. 1–4.

[33] S. T. Dawkins, J. J. McFerran, and A. N. Luiten, "Considerations on the measurement of the stability of oscillators with frequency counters," *IEEE Trans. Ultrasonics, Ferroelect. Freq. Control*, vol. 54, no. 5, pp. 918–925, May 2007.

[34] B. Wang *et al.*, "Precise and continuous time and frequency synchronisation at the 5×10^{-19} accuracy level," *Sci. Rep.*, vol. 2, no. 1, pp. 1–5, 2012.

[35] O. Lopez, A. Amy-Klein, M. Lours, C. Chardonnet, and G. J. A. P. B. Santarelli, "High-resolution microwave frequency dissemination on an 86-km urban optical link," *Appl. Phys. B*, vol. 98, no. 4, pp. 723–727, 2010.